JOC Article

A Novel Method for the Determination of Stereochemistry in Six-Membered Chairlike Rings Using Residual Dipolar Couplings

Jiangli Yan, Allen D. Kline, Huaping Mo, Michael J. Shapiro,* and Edward R. Zartler

Discovery Chemistry Research and Technologies, Lilly Research Labs, Lilly Corporate Center, Eli Lilly & Company, Indianapolis, Indiana 46285

shapiro_michael@lilly.com

Received October 25, 2002

A novel method for the determination of the relative stereochemistry of six-membered chairlike ring molecules by residual dipolar couplings is presented. C−H residual dipolar couplings were used to investigate the relative stereochemistry of 4,6-*O*-ethylidene-D-glucopyranose. For this and similar systems it is not necessary to acquire redundant dipolar couplings and to calculate the orientation order tensor. The presented methodology is a paradigmatic leap for the determination of the relative stereochemistry or remote stereochemistry in this kind of fused ring system. Residual dipolar coupling data were collected by 1D and 2D direct-measurement heteronuclear multiple quantum coherence (HMQC) spectroscopy. It was demonstrated that direct measurement of HMQC was quick and accurate for small molecules at natural abundance.

Introduction

The determination of the stereochemistry of organic molecules represents a major effort in medicinal chemistry, especially when one deals with remote stereochemistry problems. The determination of stereochemistry by NMR spectroscopy for most organic molecules is typically accomplished using combinations of nuclear Overhauser effects (NOEs) and short-range and long-range scalar *J* couplings.[1] The NOE and homonuclear *J* coupling analyses depend on proton bridges, i.e., protons within 5 Å or four bonds away from the stereocenter of interest. The measurement of long-range heteronuclear *J* couplings is not always favorable when the sample is not ^{13}C enriched, since the experiments, such as heteronuclear multiple bond coherence (HMBC) spectroscopy, can be time-consuming. When remote stereochemistry is investigated, multiple NOE or *J* coupling connections have to be performed in series to transverse the entire molecule. The further away the stereocenters are from each other, the greater number of necessary connections. These workhorse methods fail when stereochemistry is investigated if the molecule has a dearth of protons. We propose to circumvent this problem by using another information-rich NMR parameter, residual dipolar couplings (RDCs). Homo- and heteronuclear RDCs in conjunction with order matrix calculations can supply all the information necessary for the determination of a complete structure,[2−6] including stereochemistry. As presented in this paper, in the family of six-membered chairlike ring compounds, such as cyclic decalins, oligosaccharides, sterioids, alkaloids, etc., RDCs can be used to determine the relative stereochemistry without further calculation of the order tensor. Instead of multiple connections of NOEs and *J* couplings, the relative stereochemistry of six-membered chairlike ring compounds can be obtained with one measurement of C−H RDCs.

Residual dipolar couplings were first observed in solution by NMR in the 1960s.[7] These early studies focused on organic liquid crystals which produced very large dipolar couplings, and were difficult to analyze. Subsequent studies, by many groups, notably Bothner-By's, used the molecule's magnetic susceptibility anisotropy (diamagnetic at first, later paramagnetic), yielding a smaller degree of alignment and smaller couplings.[8−10] The RDCs observed in these studies were used to get structural information on small magnetically anisotropic molecules. Since the 1990s, RDCs have been measured for biomolecules partially aligned by using liquid crystals.[2,11−15] RDCs have been widely applied in

* To whom correspondence should be addressed.

(1) Neri, P.; Tringali, C. Applications of modern NMR techniques in the structural elucidation of bioactive natural products. *Bioact. Compd. Nat. Sources* **2001**, 69−127.

(2) de Alba, E.; Tjandra, N. NMR Dipolar Couplings for the Structure Determination of Biopolymers in Solution. *Prog. Nucl. Magn. Reson.* **2002**, *40*, 175−197.

(3) Prestegard, J. H.; Orientational constraints of polypeptide folds: The role of NMR in structural genomics. *Polym. Prepr. (Am. Chem. Soc., Div. Polym. Chem.* **2001**, *42*, 60.

(4) Bax, A.; Kontaxis, G.; Tjandra, N. Dipolar couplings in macromolecular structure determination. *Methods Enzymol.* **2001**, *339*, 127−174.

(5) MacDonald, D.; Lu, P. Residual dipolar couplings in nucleic acid structure determination. *Curr. Opin. Struct. Biol.* **2002**, *12*, 337−343.

(6) Brunner, E.; Residual dipolar couplings in protein NMR. *Concepts Magn. Reson.* **2001**, *13*, 238−259.

(7) Saupe, A.; Englert, G. High-resolution nuclear magnetic resonance (N.M.R.) spectra of orientated molecules. *Phys. Rev. Lett.* **1963**, *11*, 462−464.

(8) Lohman, J. A. B.; MacLean, C. Alignment effects on high resolution NMR spectra, induced by the magnetic field. *Chem. Phys.* **1978**, *35*, 269−274.

(9) Bothner-By, A. A.; Domaille, P. J.; Gayathri, C. Ultra-high field NMR spectroscopy: observation of proton-proton dipolar coupling in paramagnetic bis[tolyltris(pyrazolyl)borato]cobalt(II). *J. Am. Chem. Soc.* **1981**, *103*, 5602−5603.

(10) Lisicki, M. A.; Mishra, P. K.; Bothner-By, A. A.; Lindsey, J. S. Solution conformation of a porphyrin-quinone cage molecule determined by dipolar magnetic field effects in ultra-high-field NMR. *J. Phys. Chem.* **1988**, *92*, 3400−3403.

10.1021/jo020670i CCC: $25.00

Published on Web 02/07/2003

the structural determination of proteins,[6] nucleic acids,[5] and biopolymers[2] and for studying molecular dynamics.[16]

Residual dipolar coupling between two directly coupled nuclei, A and B, can be simply described by eq 1 in the molecular frame,[17−19] where θ denotes the angle between

$$D^{AB}(\theta,\phi) = -\frac{\mu_0 h}{16\pi^3}\gamma_A\gamma_B\left\{D_a^{AB}(3\cos^2\theta - 1) + \frac{3}{2}D_r^{AB}(\sin^2\theta\cos 2\phi)\right\}SA_a\langle r_{AB}^{-3}\rangle \quad (1)$$

the A−B interatomic vector and the z axis of the order tensor, ϕ is the angle which describes the position of the projection of the A−B interatomic vector on the $x-y$ plane, relative to the x axis, γ_A and γ_B are the gyromagnetic ratios of each interacting nucleus, D_a^{AB} and D_r^{AB} in units of hertz are the axial and rhombic components of the order tensor, A_a is the unitless axial component of the molecular alignment tensor, S is the generalized order parameter, r_{AB} is the A−B distance, and the angular brackets indicate motional averaging due to molecular tumbling. The power of RDCs is that the angular terms of eq 1 can be exploited for structural studies as well. The distance dependence of RDCs is r^{-3} and therefore allows longer-range internuclear interactions to be monitored and to provide additional distance information in addition to NOEs. RDCs are not limited to ^{1}H−^{1}H interactions, and can also be monitored for a wide range of nuclei, e.g., ^{1}H−^{13}C, ^{13}C−^{15}N, ^{1}H−^{15}N, etc.

Despite the blossoming use of RDCs in biological systems, the utility of this technique for organic molecule structure determination has not been explored extensively. Recently, RDCs have been exploited in the structural determination of carbohydrates[20−23] and have also been used to investigate the continuous bond rotation of methoxybenzene compounds.[24] All these structural determinations were obtained in combination with detailed calculation of the order tensors. H−H RDCs were measured in addition to C−H RDCs to exceed the minimum number of independent RDCs necessary for the order matrix analysis. To obtain the order matrix elements, five equations for each rigid subunit have to be solved simultaneously; therefore a minimum of 5, typically 10−15, independent RDCs are necessary for the order matrix analysis.[20−23]

We propose to use the similarity of C−H RDCs to determine the relative stereochemistry of six-membered chairlike ring compounds without further calculation of the order tensor. This idea was tested on a model molecule, 4,6-*O*-ethylidene-D-glucopyranose. In a six-membered chairlike ring fragment, each C−H or C−X bond has only two orientations relative to the ring, axial or equatorial. All the axial C−H and C−X bonds within one ring or multiple flat chair rings are parallel, or roughly so. According to eq 1, all the parallel C−H/C−X vectors which have the same angles of θ and ϕ should have the same normalized RDC values, while similarity of RDCs does not necessarily correspond to parallel vectors. Since there are only two orientations for each of the C−H/C−X bonds in the six-membered chairlike ring fragments, the similarity of the one-bond C−H RDCs, which cannot be counted as independent RDCs for the calculation of the order tensor, implies the relative orientation of C−H/C−X vectors and can bridge the relative stereochemistry. Six-membered chairlike rings are one of the basic fragments of many organic compounds and natural products. The relative stereochemistry of these compounds is important to understand their structural and functional relationship. Without rigorous mathematical manipulation and time-consuming experiments, it is now possible to determine the relative stereochemistry or remote stereochemistry of six-membered chairlike ring fragments in an aligned organic molecule. Fulfilling the promise of using RDCs in small molecules first glimpsed by Saupe,[7] we present a quick and easy method for the determination of relative structural elements in six-membered chairlike ring and similar molecules.

Results and Discussion

Measurement of Residual Dipolar Couplings of Small Molecules at Natural Abundance by Direct Heteronuclear Multiple Quantum Coherence (HMQC) Spectroscopy Experiments. A simple spin−echo pulse sequence of the 1D and 2D HMQC experiment[25], as shown in Figure 1, was slightly modified to detect the ^{13}C satellites in the ^{1}H dimension. Figure

(11) Ram, P.; Prestegard, J. H. MagneticField Induced Ordering of Bile Salt/Phospholipid Micelles: New Media for NMR Structural Investigations. *Biochim. Biophys. Acta* **1988**, *940*, 289−294.

(12) Sanders, C. R., II; Prestegard, J. H. Magnetically orientable phospholipid bilayers containing small amounts of a bile salt analog, CHAPSO. *Biophys. J.* **1990**, *58*, 447−460.

(13) Tolman, J. R.; Flanagan, J. M.; Kennedy, M. A.; Prestegard, J. H. Nuclear Magnetic Dipole Interactions in Field-Oriented Proteins: Information for Structure Determination in Solution. *Proc. Natl. Acad. Sci. U.S.A.* **1995**, *92*, 9279−9283.

(14) Tjandra, N.; Grzesiek, S.; Bax, A. Magnetic Field Dependence of Nitrogen-Proton J Splittings in ^{15}N-Enriched Human Ubiquitin Resulting from Relaxation Interference and Residual Dipolar Coupling. *J. Am. Chem. Soc.* **1996**, *118*, 6264−6272.

(15) Tjandra, N.; Bax, A. Direct measurement of distances and angles in biomolecules by NMR in a dilute liquid crystalline medium. *Science* **1997**, *278*, 1111−1114.

(16) Tolman, J. R. Dipolar couplings as a probe of molecular dynamics and structure in solution. *Curr. Opin. Struct. Biol.* **2001**, *11*, 532−539.

(17) Clore, G. M.; Gronenborn, A. M.; Bax, A. A robust method for determining the magnitude of the fully asymmetric alignment tensor of oriented macromolecules in the absence of structural information. *J. Magn. Reson.* **1998**, *133*, 216−221.

(18) Clore, G. M.; Gronenborn, A. M.; Tjandra, N. Direct structure refinement against residual dipolar couplings in the presence of rhombicity of unknown magnitude. *J. Magn. Reson.* **1998**, *131*, 159−162.

(19) Bax, A.; Tjandra, N. High-resolution heteronuclear NMR of human ubiquitin in an aqueous liquid crystalline medium. *J. Biol. NMR* **1997**, *10*, 289−292.

(20) Neubauer, H.; Meiler, J.; Peti, W.; Griesinger, C. NMR structure determination of saccharose and raffinose by means of homo- and heteronuclear dipolar couplings. *Helv. Chim. Acta* **2001**, *84*, 243−258.

(21) Freedberg, D. I.; An Alternative Method for Pucker Determination in Carbohydrates from Residual Dipolar Couplings: A Solution NMR Study of the Fructofuranosyl Ring of Sucrose. *J. Am. Chem. Soc.* **2002**, *124*, 2358−2362.

(22) Azurmendi, H. F.; Bush, C. A. Conformational studies of blood group A and blood group B oligosaccharides using NMR residual dipolar couplings. *Carbohydr. Res.* **2002**, *337*, 905−915.

(23) Martin-Pastor, M.; Bush, C. A. Conformational Studies of Human Milk Oligosaccharides Using 1H-13C One-Bond NMR Residual Dipolar Couplings. *Biochemistry* **2000**, *39*, 4674−4683.

(24) Emsley, J. W.; Foord, E. K.; Lindon, J. C. Continuous bond rotation models for the conformational analysis of the methoxy groups in 1,2-dimethoxy- and 1,2,3-trimethoxy-benzene using dipolar couplings obtained from the NMR spectra of oriented samples in nematic liquid crystalline solutions. *J. Chem. Soc., Perkin Trans. 2* **1998**, *5*, 1211−1218.

(25) Bax, A.; Griffey, R. H.; Hawkins, B. L. Correlation of proton and nitrogen-15 chemical shifts by multiple quantum NMR. *J. Magn. Reson.* **1983**, *55*, 301−315.

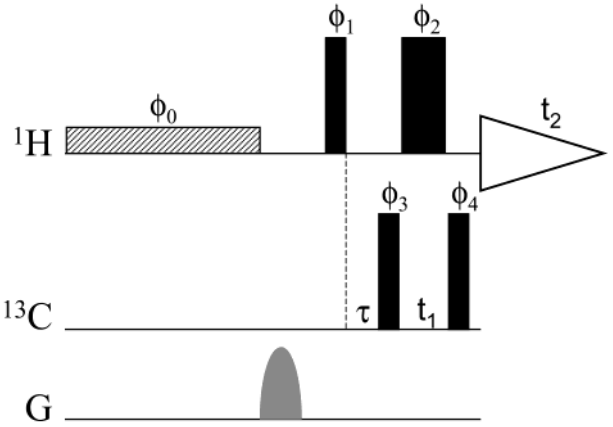

FIGURE 1. Pulse sequence scheme of HMQC experiments for the measurement of CH dipolar couplings. Narrow and wide bars denote $\pi/2$ and π pulses. Two carbon $\pi/2$ pulses are symmetrically centered at the proton π pulse. The INEPT delay τ is $1/2J_{CH}$. Before excitation, presaturation with a small gradient was applied to suppress the water. Phase cycling: $\phi_0 = x$, $\phi_1 = x$, $\phi_2 = x$, $\phi_3 = x, -x$, $\phi_4 = x, x, -x, -x$, and $\phi_{rec.} = x, -x, -x, x$.

2A displays the 1D HMQC spectrum of lactose with 10 mg/mL phage recorded by the modified pulse sequence. It is clear that the resolution for the anomeric protons is good, but the signals of other protons are heavily overlapped. For some simple molecules, this 1D HMQC may be sufficient to measure RDCs. However, for molecules that are spectrally complex, greater spectral dispersion is required. A fast 2D HMQC without $^1H-^{13}C$ decoupling during acquisition was used to measure scalar and residual dipolar couplings. There is no need for high digital resolution in the ^{13}C dimension since the measurements occur in the direct dimension. In practice, a proton spectral width of 2400 Hz (4 ppm) and acquisition time of 3.41 s were used to keep the high resolution of the F_2 dimension, while carbon parameters were set to a minimum to obtain sufficient resolution to eliminate overlap of resonances within a minimum of acquisition time. With the exception of the C4−H4 signal of glucose, the other signals of all three rings, which were heavily overlapped in the 1D spectrum (Figure 2A), are well dispersed (Figure 2B). The ^1H and ^{13}C chemical shift assignments, shown in Figure 2, were obtained using homonuclear total correlation spectroscopy (TOCSY), homonuclear correlation spectroscopy (COSY), and HMQC and also agreed with the literature values.[26] The chemical shifts of both H4 and C4 of both glucose anomers are the same. The RDCs of lactose were measured using the 2D HMQC sequence and samples with 10 or 14 mg/mL phage (Table 1). The HMQC experiment for the 10 mg/mL phage sample was repeated three times; the root-mean-square deviation (rmsd) shown in Table 1 indicates that the direct measurement method precision is at the level of FID resolution.

Constant-time heteronuclear single quantum coherence (CT-HSQC)[27,28] has been widely used to measure RDCs for the structure determinations of proteins and

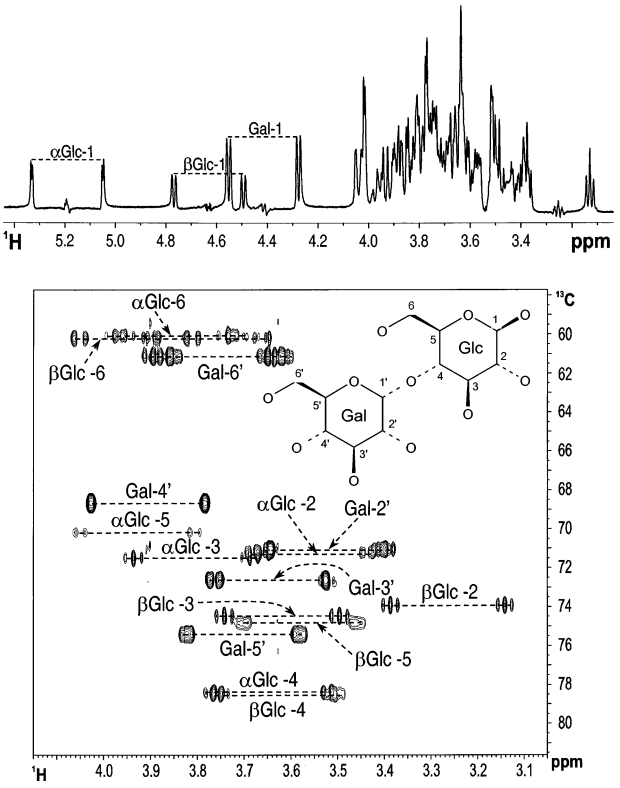

FIGURE 2. (A, top) 1D $^1H-^{13}C$ HMQC spectrum for direct measurement of dipolar couplings of lactose. (B, bottom) Expanded 2D $^1H-^{13}C$ HMQC spectrum for direct measurement of dipolar couplings of lactose. The FIDs for both (A) and (B) were acquired in 16K data points over a spectral width of 2400 Hz in the proton dimension. A total of 64 data points were collected in the carbon dimension with a spectral width of 3600 Hz. An INEPT delay of 3.12 ms corresponding to a J constant of 160 Hz was used for the 2D HMQC (B). Spectra were recorded at 298 K with 300 mM lactose and 10 mg/mL pf1 phage in D_2O. The assignments of all the signals are labeled.

nucleic acids.[29] Constant time can eliminate the C−C coupling and generate high-resolution spectra after application of linear prediction. CT-HSQC was utilized to measure the $^1H-^{13}C$ RDCs of lactose in the indirect dimension. Figure 3 displays a spectrum collected with 300 mM lactose in 100% D_2O containing 10 mg/mL Pf1 phage. A linear prediction by 50% and a zero-filling by a factor of 8 in the ^{13}C dimension were used to process the CT-HSQC spectra. The measured RDCs are listed in Table 1. A comparison of the RDCs measured by direct-dimension measurement (HMQC) and indirect-dimension measurement (CT-HSQC) is also shown. The indirect method can be used in this case, but the errors due to digital resolution can be substantial if the RDC is small. In addition, the direct measurement is much less time consuming; it takes at least 2 times as long to perform the CT-HSQC than the direct HMQC with the same

(26) Nunez, H. A.; Barker, R. Enzymic synthesis and carbon-13 nuclear magnetic resonance conformational studies of disaccharides containing b-D-galactopyranosyl and b-D-[1-13C]galactopyranosyl residues. *Biochemistry* **1980**, *19*, 489−495.

(27) Vuister, G. W.; Bax, A. Resolution enhancement and spectral editing of uniformly carbon-13-enriched proteins by homonuclear broadband carbon-13 decoupling. *J. Magn. Reson.* **1992**, *98*, 428−435.

(28) Hallenga, K.; Lippens, G. M. A constant-time 13C-1H HSOC with uniform excitation over the complete 13C chemical shift range. *J. Biomol. NMR* **1995**, *5*, 59−66.

(29) Mittermaier, A.; Kay, L. E. c1 Torsion angle dynamics in proteins from dipolar couplings. *J. Am. Chem. Soc.* **2001**, *123*, 6892−6903.

TABLE 1. Residual Dipolar Coupling Constants of Lactose Measured by 2D HMQC and CT-HSQC Experiments

		direct HMQC		indirect CT-HSQC
res	no.	RDC_{10}/Hz, 10 mg/mL phage	RDC_{14}/Hz, 14 mg/mL phage	RDC_{10}/Hz, 10 mg/mL phage
Gal	1′	3.05 ± 0.10	4.26	2.32 ± 0.33
	2′	2.23 ± 0.13	3.32	1.62 ± 1.25
	3′	2.14 ± 0.12	3.25	3.32 ± 0.59
	4′	−0.39 ± 0.06	−0.54	−1.40 ± 0.15
	5′	3.08 ± 0.09	4.33	3.98 ± 0.44
α-Glc	1	−1.39 ± 0.02	−1.98	−2.99 ± 0.55
	2	2.63 ± 0.16	2.91	4.05 ± 0
	3	2.62 ± 0.10	3.65	3.10 ± 0.22
	4[a]			
	5	2.44 ± 0.19	3.11	3.50 ± 0.41
β-Glc	1	2.67 ± 0.11	3.57	3.28 ± 0.55
	2[b]	2.52 ± 0.05	3.32	1.25 ± 1.11
	3	2.85 ± 0.07	3.60	3.12 ± 0.10
	4[a]			
	5	2.66 ± 0.16	3.31	3.70 ± 0.11

[a] The ^1H and ^{13}C chemical shifts of two glucose C4−H4 vectors are the same. RDCs of these two vectors could not be measured. [b] H2 of β-Glu1 is partially overlapped with H2′ of Gal, and its RDC was measured using a single peak.

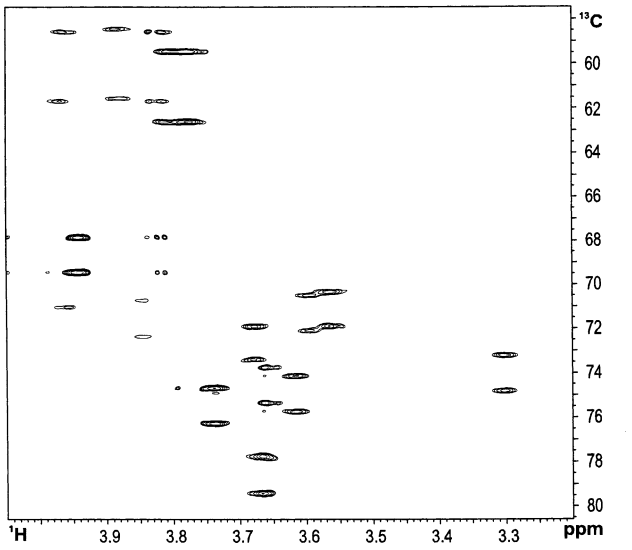

FIGURE 3. Expanded 2D $^1H-^{13}C$ CT-HSQC spectrum for indirect measurement of dipolar couplings of lactose at 298 K. The experiment was performed with 1k × 512 points to cover a sweep width of 2404 Hz × 6037 Hz in F_2 (^1H) and F_1 (^{13}C). The sample is the same as described in Figure 2.

resolution. Since small molecules are more difficult to align than biomolecules, the deviation in the indirect measurement of small RDCs will be unfavorable. At low concentrations, the acquisition time for indirect measurement using natural abundance samples becomes unfavorable too. However, peaks in the CT-HSQC are more easily analyzed, while measurements in direct HMQC need more careful data analysis.[30]

The inconvenience in the peak definition with direct HMQC measurement is caused by complicated multiplets resulting from H−H couplings and asymmetries of line shapes. Besides the C−H splitting, short-range and long-range (≥3 bonds) homonuclear *J* and *D* couplings also show up in the H observed measurement and give rise

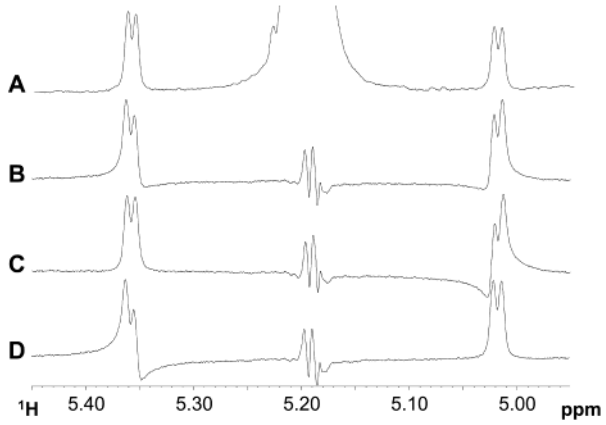

FIGURE 4. Two satellites of α-Glc-1 on the expanded 1D ^1H spectrum (A), 1D HMQC spectrum phased by the entire spectrum (B), 1D HMQC spectrum phased by the downfield satellite at 5.36 ppm (C), and 1D HMQC spectrum phased by the upfield satellite at 5.02 ppm (D). The FIDs for both experiments were acquired in 16K data points over a spectral width of 2400 Hz in the proton dimension. An INEPT delay of 3.45 ms corresponding to a *J* constant of 145 Hz was used for the 1D HMQC. Spectra were recorded at 298 K with 300 mM lactose in D_2O.

to highly complex multiplets, especially for the oriented sample. This results in a decrease of the signal-to-noise ratio and difficulties in accurately defining the peak. In addition, the two ^{13}C satellites are not symmetric since the measured *J* value is sensitive to the nonsymmetric line shape,[31] as observed in our experiments (Figure 2). The phase distortion of each satellite due to line-shape asymmetry introduces deviations to the scalar coupling and residual dipolar coupling measurements. The deviation of individual signals depends on the difference between the real *J* value of the signal and the experimental *J* constant corresponding to the INEPT delay. But it was found by using the satellites on the 1D spectra that the effect of the asymmetric line shape could be corrected by phasing individual satellites and measuring their frequencies independently. Figure 4 shows the comparison of the two satellites of lactose α-Glc-1 on the 1D proton spectrum (Figure 4A) and on the 1D HMQC spectrum (Figure 4B). The phase distortion was clearly observed in Figure 4B. The frequency difference of the satellites is 169.82 Hz measured from Figure 4A and 170.52 Hz from Figure 4B. The data of two well-dispersed signals, those of α-Glc-1 and Gal-1, measured at different conditions are presented in Table 2. The signal of β-Glc-1 was not used for the comparison since its downfield satellite was too close to the very strong central signal of Gal-1′. Using the satellites on the 1D proton spectrum as a reference, the phase distortion in the HMQC experiment enhanced the measured splitting and introduced an error of 0.20−0.60 Hz into the *J* or $J + D$ detections when a 160 Hz *J* constant (corresponding to an INEPT delay of 3.12 ms) was used to record the

(30) Andrec, M.; Prestegard, J. H. A metropolis Monte Carlo implementation of Bayesian time-domain parameter estimation: application to coupling constant estimation from antiphase multiplets. *J. Magn. Reson.* **1998**, *130*, 217−232.

(31) Tjandra, N.; Bax, A. Measurement of dipolar contributions to 1JCH splittings from magnetic-field dependence of J modulation in two-dimensional NMR spectra. *J. Magn. Reson.* **1997**, *124*, 512−515.

TABLE 2. Scalar and Dipolar Splitting of ^{13}C Satellites of α-Glc-1 and Gal-1′

			splitting of satellites[a] (Hz)			difference[b] (Hz)		
sample	method	proton	1D ^1H	spectral phasing	1 by 1 phasing	spectral phasing	1 by 1 phasing	*J* constant for HMQC (Hz)
isotropic	1D HMQC	α-Glc- 1	169.82	170.52	169.89	0.70	0.07	145[c]
		Gal-1	162.07	162.73	162.09	0.66	0.02	
isotropic	1D HMQC	α-Glc- 1	169.90	170.24	169.90	0.34	0.00	160[d]
		Gal-1	162.15	162.38	162.15	0.23	0.00	
	2D HMQC	α-Glc- 1	169.90	170.20	169.94	0.30	0.04	
		Gal-1	162.15	162.35	162.20	0.20	0.05	
aligned	1D HMQC	α-Glc- 1	168.40	168.79	168.45	0.39	0.05	160[e]
		Gal-1	165.16	165.68	165.11	0.52	−0.05	
	1D HMQC	α-Glc- 1	168.40	168.77	168.42	0.37	0.02	
		Gal-1	165.16	165.70	165.19	0.54	0.03	
	2D HMQC	α-Glc- 1	168.40	168.97	168.46	0.57	0.06	
		Gal-1	165.16	165.70	165.23	0.54	0.07	
	2D HMQC	α-Glc- 1	168.40	169.00	168.49	0.60	0.09	
		Gal-1	165.16	165.73	165.11	0.57	−0.02	

[a] The present data were the average from two doublet peaks of each satellite. [b] The difference here represents the subtraction of HMQC splitting and the reference splitting. [c] Both 1D regular and HMQC spectra were collected with high FID resolution of 0.075 Hz per point; the INEPT delay of the 1D HMQC experiment was set to 3.45 ms corresponding to a *J* constant of 145 Hz. [d] The FID resolution of all the listed experiments is 0.29 Hz per point; the INEPT delay of the HMQC experiment was set to 3.12 ms corresponding to a *J* constant of 160 Hz. [e] The FID resolution of all the listed experiments is 0.29 Hz per point. Two repeated data for the 1D and 2D HMQC experiments are shown. The INEPT delay of the HMQC experiment was set to 3.12 ms corresponding to a *J* constant of 160 Hz.

HMQC spectra. The error increased to 0.70 and 0.66 Hz for α-Glc-1 (also see Figure 4A,B) and Gal-1 signals, respectively, when a 145 Hz *J* constant (corresponding to an INEPT delay of 3.45 ms) was used, since 145 Hz is further from the real splitting of these two signals than 160 Hz. It is impossible to set a *J* constant to match every observed signal. Therefore, it is advised not to phase the total spectrum and do automatic peak-picking for the RDC measurement by direct HMQC. In this paper, the pair of ^{13}C satellites on the H dimension for individual C−H vectors was sliced from the 2D HMQC first, each satellite of the pair was phased independently, and the frequencies of its multiplets were measured. As an example in Figure 4, the downfield satellite of α-Glc-1 was phased and the frequencies of the doublet of this satellite were measured first (Figure 4C). The upfield satellite was then phased and peak-picked (Figure 4D). The satellite splitting was calculated from the frequencies measured in Figure 3C,D. The datum 169.89 Hz listed in Table 2 was the average of two frequency differences of the α-Glc-1 doublets. As shown in Table 2, the deviations of the measured splitting of the satellites on the 1D proton spectrum and HMQC experiment dropped to zero after the phase correction was performed on each of the satellites independently. The independent phase correction of each signal yields accurate measurement of scalar couplings and residual dipolar couplings in the ^1H dimension of HMQC experiments. Since only a limited number of signals are analyzed, this is a practical method to measure scalar couplings and residual dipolar couplings of small molecules. The *J* or $J + D$ coupling was the average of the values measured on all multiplets; the measurement error from the multiplets was within the FID resolution, as shown in Table 2. The RDC was the subtraction of the splitting of the aligned sample from the splitting of the isotropic sample. Therefore, direct HMQC is a reliable, fast, and easy method to measure the RDCs for small molecules at natural abundance.

Bicelles[15,32,33] and bacteriophages[34−37] are the two most widely used media to partially align biomolecules.[2−4,38−41] We found that they are also good media to partially align lactose. With 10% bicelles (DMPC:DHPC = 2.8:1, molar ratio), we measured RDCs of 4.70, 3.81, and −2.05 Hz for the anomeric $^1H-^{13}C$ vectors of galactose and two glucose isomers, respectively. With 10 mg/mL Pf1 phage, we measured 3.08, 2.93, and −1.03 Hz for the $^1H-^{13}C$ vectors for the galactose and two glucose anomeric protons. When 14 mg/mL phage was used, the RDCs of the three anomeric $^1H-^{13}C$ vectors increased to 4.55, 3.96, and −1.85 Hz, respectively. The *J* couplings of three anomeric signals measured by HMQC at room temperature in bicelle samples and an isotropic sample (without phage) are consistent with each other (the maximum

(32) Ottiger, M.; Bax, A. Characterization of magnetically oriented phospholipid micelles for measurement of dipolar couplings in macromolecules. *J. Biomol. NMR* **1998**, *12*, 361−372.
(33) Losonczi, J. A.; Prestegard, J. H. Improved dilute bicelle solutions for high-resolution NMR of biological macromolecules. *J. Biomol. NMR* **1998**, *12*, 447−451.
(34) Hansen, M. R.; Mueller, L.; Pardi, A. Tunable alignment of macromolecules by filamentous phage yields dipolar coupling interactions. *Nat. Stuct. Biol.* **1998**, *5*, 1065−1074.
(35) Trempe, J.-F.; Morin, F. G.; Xia, Z.; Marchessault, R. H.; Gehring, K. Characterization of polyacrylamide-stabilized Pf1 phage liquid crystals for protein NMR spectroscopy. *J. Biol. NMR* **2002**, *22*, 83−87.
(36) Zweckstetter, M.; Bax, A. Characterization of molecular alignment in aqueous suspensions of Pf1 bacteriophage. *J. Biol. NMR* **2001**, *20*, 365−377.
(37) Barrientos, L. G.; Louis, J. M.; Gronenborn, A. M. Characterization of the cholesteric phase of filamentous bacteriophage fd for molecular alignment. *J. Magn. Reson.* **2001**, *149*, 154−158.
(38) Prestegard, J. H.; New Techniques in Structural NMR− Anisotropic Interactions. *Nat. Struct. Biol.* **1998**, NMR Suppl., 517−522.
(39) Prestegard, J. H.; Al-Hashimi, H. M.; Tolman, J. R. NMR structures of biomolecules using field oriented media and residual dipolar couplings. *Q. Rev. Biophys.* **2000**, *33*, 371−424.
(40) Pan, B.; Li, B.; Russell, S. J.; Tom, J. Y. K.; Cochran, A. G.; Fairbrother, W. J. Solution Structure of a Phage-derived Peptide Antagonist in Complex with Vascular Endothelial Growth Factor. *J. Mol. Biol.* **2002**, *316*, 769−787.
(41) Sibille, N.; Pardi, A.; Simorre, J.-P.; Blackledge, M. Refinement of Local and Long-Range Structural Order in Theophylline-Binding RNA Using 13C-1H Residual Dipolar Couplings and Restrained Molecular Dynamics. *J. Am. Chem. Soc.* **2001**, *123*, 12135−12146.

deviation is 0.19 Hz). The consistency of the measurements with different samples indicates the direct HMQC method for the RDCs is accurate.

Determination of the Stereochemistry of 4,6-*O*-Ethylidene-D-glucopyranose by Residual Dipolar Couplings Only. The angular terms in eq 1 have been exploited widely in the structural determination of biomolecules. The structure of a small molecule can also be determined in this way. For this purpose, order matrix analysis is necessary to generate an order tensor for each rigid moiety and to extract a full measure of structural information encoded in RDCs. However, at least 5 (usually 10−15) independent RDCs are required for each rigid subunit, and several experiments are needed to collect different types of RDCs, such as one bond and multiple bond $^{13}C-^{1}H$ and $^{1}H-^{1}H$. Complete structural information is not always necessary for all compounds; e.g., only relative or absolute stereochemistry is desired. While calculation of the order tensor may be needed for the determination of absolute stereochemistry, the real angles between each internuclear vector and the order tensor, θ and ϕ, are not really necessary for some relative orientations. If an orientation reference in a rigid or pseudorigid fragment can be found, the RDCs should give information on the relative angles to the reference without further calculation of the order tensor.

Six-membered chairlike rings are the building blocks of many important families, such as oligosaccharides, steroids, and alkaloids. In six-membered chair or multiple-chair moieties, all the axial C−H vectors are parallel or close to parallel. According to eq 1, the parallel vectors must have the same RDCs since they have the same angles of θ and ϕ relative to the order tensor. But the reverse is not necessarily true; the similarity of the RDC values does not necessarily mean that the corresponding vectors are parallel. In this particular molecule and many other six-membered chairlike rings, all the protons or other groups on the ring have only two orientations, axial or equatorial, relative to the ring. The axial vectors must have similar RDCs, while the equatorial C−H vectors may have different values. In some unfortunate cases, one of the equatorial C−H vectors may have an RDC value similar to the values of axial C−H vectors, which means this equatorial C−H vector may have the same angles to the order tensor as all the axial C−H vectors, including the C−H or C−X vector at the same carbon. The possibility for several unparallel vectors within a small molecule having the same angles to the order tensor is unlikely and thus can be ignored. If measured RDCs of two interatomic vectors (not necessarily the same type) at one carbon are different, one with an RDC value similar to that of the known axial reference has to be axial and the other must be equatorial. Therefore, the similarity of the RDCs implies the same relative orientations. The RDCs of parallel C−H vectors may not be applicable for structural calculation since they cannot be really counted as independent values for calculation of the order tensor, but they are very useful in determination of the relative orientations in this kind of compound. This idea to simply determine the stereochemistry or remote stereochemistry of six-membered chairlike ring compounds by RDCs without the calculation of the order tensor was tested using 4,6-*O*-ethylidene-D-glucopyranose (4,6-*O*-ethylidene-D-glucose, 4,6-*O*-EGP) as a model.

TABLE 3. ^{1}H and ^{13}C Chemical Shifts of 4,6-*O*-EGP

	^{1}H chemical shift/ppm		^{13}C chemical shift/ppm	
position	isomer A	isomer B	isomer A	isomer B
1	4.71	5.23	93.4	97.1
2	3.29	3.66	72.6	75.5
3	3.64	3.82	70.3	73.1
4	3.47	3.42	80.5	80.0
5	3.47	3.85	62.6	66.5
6	4.18	4.12	68.3	67.9
	3.64	3.63		
7	4.88	4.89	100.4	100.4

4,6-*O*-EGP is a specific inhibitor at the outer surface of a glucose transporter in various membrane cells.[42,43] It is a basic reagent of many antitumor drugs[44] and biologically active compounds.[45] 4,6-*O*-EGP undergoes slow conformational exchange in solution due to flipping of the anomeric proton at the reducing end of the glucose ring; two conformers are designated as the major isomer (A) and minor isomer (B). Two anomeric signals at 5.23 and 4.71 ppm were observed by ^{1}H NMR (Figure 5). The population ratio of A:B at 303 K is 70:30. Except the H-7 and C-7 peaks, all peaks of the two isomers were well dispersed in the 2D HMQC spectrum (Figure 6). The ^{1}H and ^{13}C chemical shifts, shown in Table 3, were assigned by analysis of 2D COSY and HMQC. No difference in the ^{13}C chemical shifts of C-7 in the two forms was observed using HMQC experiments with an FID resolution of 52 Hz in the ^{13}C dimension. But in the ^{1}H dimension, the H-7 chemical shifts are slightly different, with the minor isomer's resonances around 2.5 Hz further downfield than those of the major one. Since not all the multiplets were distinguished on slices of HMQC spectra, the RDCs of C−H at position 7 were measured on the basis of one single distinguishable peak instead of the average of all the multiplets. The RDC values of C7−H7 vectors may include more deviations than the other. All measured RDC data are shown in Figure 7A, a plot of RDC vs CH position. Figure 7A indicates clear patterns of the relative orientations. In both isomers, the protons at position 7 are in axial configurations because they are proximal to a methyl at the same carbon; therefore, H-7 was chosen as the orientation reference in our study. All of the C−H vectors of the major component A except C6−H6a have very similar RDCs (within the range of 3.67−5.03 Hz). Comparison of the RDCs of C6−H6a (2.19 Hz) and C6−H6b (4.44 Hz) to the RDC of reference C7−H7 (5.03 Hz), it is obvious that H6a is equatorial and H6b is axial. In the minor isomer B, C1−H1 and C6−H6a have RDC

(42) Delicado, E.; Torres, M.; Miras-Portugal, M. T. Effects of insulin on glucose transporters and metabolic patterns in Harding-Passey melanoma cells. *Cancer Res.* **1986**, *46*, 3762−3767.

(43) Kawada, J.; Okita, M.; Nukatsuka, M.; Toyooka, K.; Naito, S.; Nabeshima, A.; Tsujihara, K.; Yoshimura, Y.; Nishida, M. Ethylidene glucose-substituted new analog of streptozotocin cannot induce diabetes: study on the basis of structure and activity relationship. *Mol. Cell. Endocrinol.* **1989**, *62*, 153−159.

(44) Naidu, R. Synthetic method for the preparation of the antineoplastic agent etoposide. PCT Int. Appl., 2000.

(45) Sah, A. K.; Rao, C. P.; Saarenketo, P. K.; Wegelius, E. K.; Rissanen, K.; Kolehmainen, E. N-Glycosylamines of 4,6-O-ethylidene-a-D-glucopyranose: synthesis, characterisation and structure of CO2H, Cl and F ortho-substituted phenyl derivatives and metal ion complexes of the CO2H derivative. *Dalton* **2000**, *20*, 3681−3687.

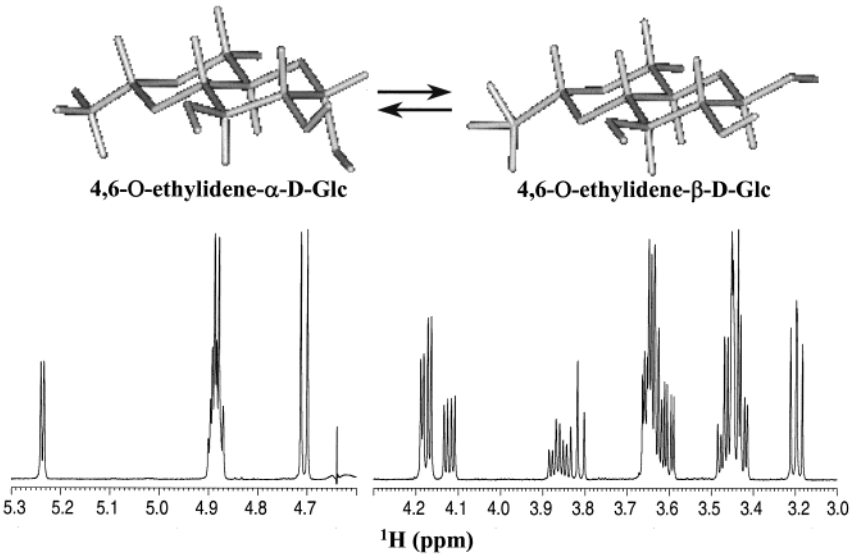

FIGURE 5. Conformational exchange of 4,6-*O*-EGP in aqueous solution observed by NMR. The anomeric peak intensity ratio of the two isomers is 70:30.

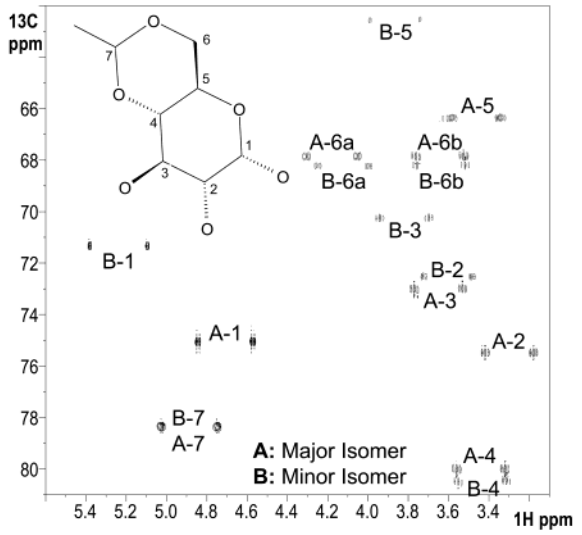

FIGURE 6. 2D $^{1}H-^{13}C$ HMQC spectrum for direct measurement of RDCs of 4,6-*O*-EGP collected with 32k × 64 points to cover a spectral window of 4808 Hz × 3320 Hz in F_2 (^{1}H) and F_1 (^{13}C). An INEPT delay of 3.12 ms corresponding to a *J* constant of 160 Hz was used. Spectra were recorded at 298 K with 10 mM 4,6-*O*-EGP and 14 mg/mL pf1 phage in PBS buffer (pD 7.3).

values (−4.96 and 2.37 Hz) very different from those of the other seven (within 5.42−5.92 Hz). The orientations of H6a (axial) and H6b (equatorial) are easily established from the data of C6−H6a (2.37 Hz), C6−H6b (5.92 Hz), and C7−H7 (reference, 5.85 Hz). By comparison of the pattern of C1−H1 to that of C7−H7 within the same molecule, the major (4.36 to 5.03 Hz) and minor (−4.98 to +5.83 Hz) isomers were unambiguously assigned to 4,6-*O*-ethylidene-α-D-glucose (E-αGlc) and 4,6-*O*-ethylidene-*β*-D-glucose (E-*β*Glc). On the basis of the consistency of C4−H4 and C5−H5 with C7−H7, C6−H6 and C2−H2, C3−H3 RDCs, the double-chair conformation was confirmed in both E-αGlc and E-*β*Glc conformers. While the C−H RDCs of each isomer are not exactly the same, we believe the reason is that these C−H bonds are not exactly parallel. The map of measured RDCs on the structures (Figure 7B) presents clear correlations between the RDCs and the relative orientations of individual C−H vectors. In summary, from the C−H RDC measurement we determined the anomeric configuration, the unambiguous assignment of two protons at C6, and the confirmation of the double-chair conformation for the two exchanging molecules simultaneously.

The routine way to get the relative stereochemistry from H7 to H1 by NMR is using NOEs and *J* couplings.[1] All the protons in the NOE linkage chain are important. The result cannot be obtained if one of the protons in the chain is missing and the NOE linkage is broken. For E-αGlc, it is necessary to have at least three connections, NOE(H7,H4), NOE(H4,H2), and NOE(H2,H1) or NOE(H7,H6*β*), NOE(H6*β*,H2), and NOE(H2,H1). For E-*β*Glc more NOE connections are needed to get the relative orientation from H7 to H1, because only the very weak NOE(H2,H1) can be detected. In solution, two exchangeable isomers, E-αGlc and E-*β*Glc, exist simultaneously. The small differences between the chemical shift of two H4 atoms and two H6*β* atoms of the α and *β* isomers result in the ambiguous usage of NOE(H7,H4) or NOE(H7,H6*β*) to go through the NOE connections from one end to another, as shown in Figure 8. The linkage via protons has the same importance in the determination of relative stereochemistry using *J* couplings. In this specific case, J_{HX} or long-range J_{HH} couplings are needed for the determination of relative stereochemistry. When RDC is applied to determine the relative stereochemistry or remote stereochemistry, it is not necessary to have a proton linkage between the investigated vectors. To get the relative orientation of H1 from H7 of 4,6-*O*-EGP, only the RDCs of C7−H7 and C1−H1 are necessary and the overlapping signals in the upfield area can be ignored. This will be very useful for multiply linked six-membered chairlike ring compounds.

To determine the relative stereochemistry or remote stereochemistry, the reference and target vectors/bonds could be any pair of nuclei (H−H, C−H, N−H, C−F, H−F, C−C, or C−N), as long as they are detectable. Figure 9 presents the plot of C−H (black solid triangles

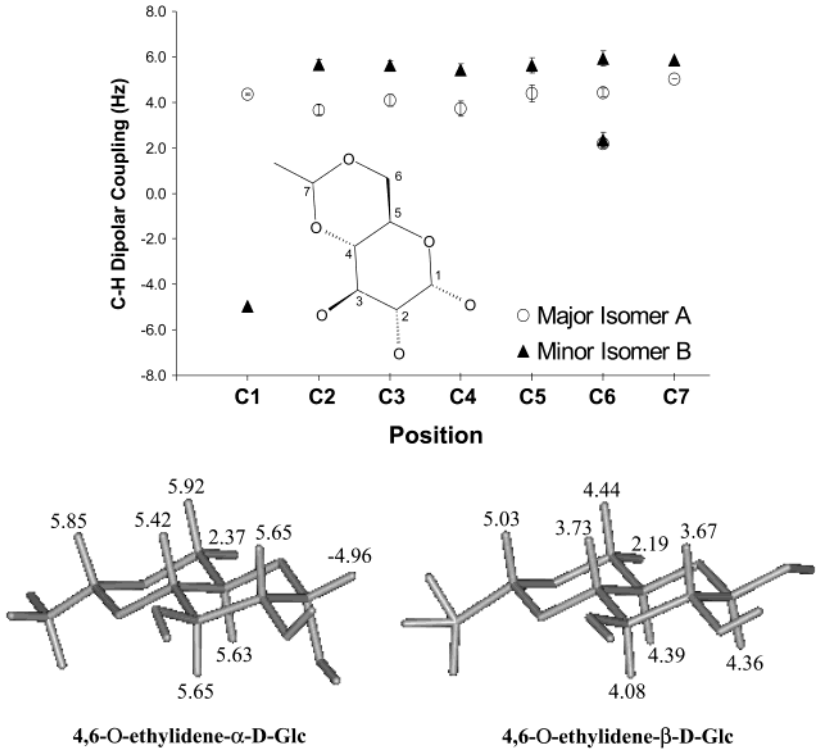

FIGURE 7. (A, top) C−H dipolar couplings of 4,6-*O*-EGP via carbon position. **(**B, bottom**)** Map of C−H dipolar couplings on structures of α- and *β*-4,6-O-EGP isomers. RDCs were measured by 2D HMQC with 14 mg/mL phage in PBS buffer (pD 7.3). The error bars in (A) are rmsd's from the measurements of multiplets of each signal. The assignment was accomplished by RDCs as well as COSY.

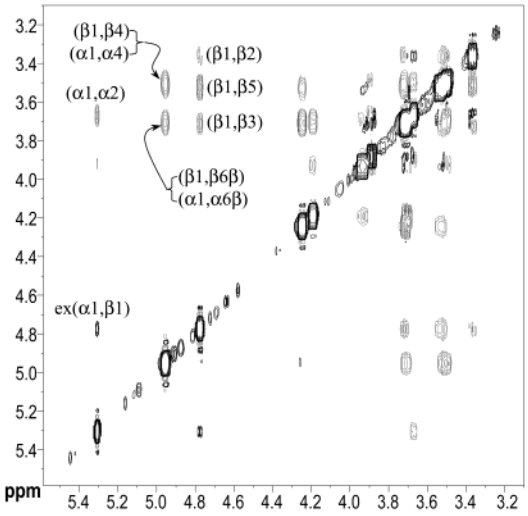

FIGURE 8. 2D NOESY spectrum of 10 mM 4,6-*O*-EGP in PBS buffer (pD 7.3). A mixing time of 1.2 s was used, while the recovery time was 2 s. A total of 1024 (t_2) × 256 (t_1) data points were recorded to cover 4808 Hz in each dimension.

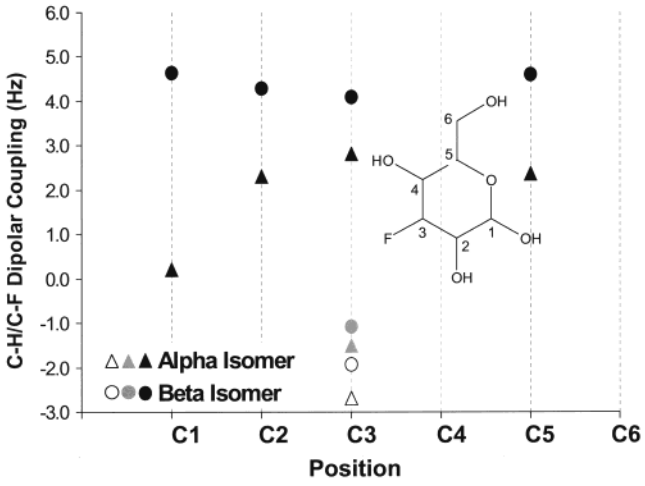

FIGURE 9. C−H (black solid circles and triangles) and C−F (open circle and triangle) RDCs of 20 mM F-Glc with 15 mg/mL phage in PBS buffer (pD 7.3) via carbon position. C−H RDCs were measured by 2D HMQC. C−F RDCs were measured by 1D ^{1}H-decoupled (NOE-enhanced) ^{13}C spectra. The C−F RDCs (open circle and triangle) were normalized to C−H RDCs (gray solid circles and triangles) by $D_{CH} = D_{CF}(\gamma_H\langle r_{CH}^{-3}\rangle)/(\gamma_F\langle r_{CF}^{-3}\rangle)$, where γ_H and γ_F are 2.6753 × 10^8 and 2.5181 × 10^8 T s^{-1} and r_{CH} and r_{CF} are 1.35 and 1.09 Å, respectively.

and circles) and C−F (open triangles and circles) RDCs vs vector position of 3-fluoro-3-deoxy-D-glucose (F-Glc). The C−H RDCs were measured from the F_2 dimension of HMQC, while the C−F RDCs were obtained from a proton-decoupled carbon experiment. For convenient comparison, the C−F RDCs were normalized to the values of C−H RDCs (gray solid triangles and circles), simply by $D_{CH} = D_{CF}(\gamma_H\langle r_{CH}^{-3}\rangle)/(\gamma_F\langle r_{CF}^{-3}\rangle)$,[17] where γ_H and γ_F are 2.6753 × 10^8 and 2.5181 × 10^8 T s^{-1} and r_{CH} and r_{CF} are 1.35 and 1.09 Å, respectively. The data show the unambiguous assignment of the α and *β* isomers and the conformation of fluorine. Fluorine in both the α and *β* isomers has an equatorial orientation, while the protons at the same carbon are axial.

The C−H RDC data of lactose in Table 1 also present clear patterns of the equatorial proton relative to the

axial protons within each six-membered chairlike ring. Lactose also undergoes slow conformational exchange in solution (β:α = 65:35). Two sets of signals were observed for the glucose ring, while only one was detected for the galactose ring. The RDCs of galactose C1−H1, C2−H2, C3−H3, and C5−H5 are very similar to each other (∼2.14−3.28 Hz using 10 mg/mL phage), but the value of C4−H4 is much different (−0.3 Hz), as would be expected. It is easy to unambiguously assign the α and β forms of glucose by only RDCs, since the key difference between α- and β-glucose is the orientation of the anomeric proton (H1) relative to other ring protons (H2, H3, H4, and H5). All the measured RDCs of C1−H1, C2−H2, C3−H3, and C5−H5 of the major isomer (β-glucose) are within 2.5−2.8 Hz, while the RDC of C1−H1 of the minor isomer (α-glucose) is −1.13 Hz, quite different from the others. It is important to know that the application of the similarity of the RDCs to determine the relative stereochemistry of six-membered chairlike ring and similar compounds is currently limited in the rigid-conformation fragments. The comparison of the RDCs of the target vector to that of the reference vector beyond the rigid moiety or beyond one molecule is not meaningful. Therefore, the similarity of axial C−H RDCs of α-glucose, β-glucose, and galactose probably is coincidental. We cannot compare either the data of α-glucose to those of β-glucose or the data of glucose to those of galactose, because different rigid fragments (even within a single molecule) have different order tensors and the relative orientations of the tensors are unknown until the calculation is finished. This is one example in which the RDCs of galactose axial C−H and glucose axial C−H are accidentally similar. The galactose data actually are the average of the data of two exchangeable isomers, and this is another reason for all the measured C−H vectors having similar RDCs. Although we cannot get the relative orientation of C−H vectors in two rings, for example, the relative orientation of C4′−H4′ of galactose to C1−H1 of glucose directly by RDCs, we know the relative orientation of C4′−H4′ to C1′−H1′ of galactose (they are both axial) and the relative orientation of C1−H1 to C4−H4 of glucose. The relative orientation of C1′−H1′ to C4−H4 therefore correlates to the relative orientation of C1′−H1′ of galactose and C4−H4 of glucose that depends on the 1′ → 4 linkage of lactose, or the glycoside dihedral angles Φ and Ψ. These angles describe the relative orientations of the individual rings and the three-dimensional structures of many oligosaccharides, therefore attracting much interest in NMR,[46−48] crystallography,[49] and molecular mechanics force field simulation.[50−53] Although the linkage is flexible, it has only a couple of low-energy conformations.[50−53] Sometimes, the linkage type can be inferred from the ^{1}H and ^{13}C chemical shifts if the specific linkage has been reported previously[46] or the low-energy conformation of molecular simulation.[50−52] RDCs cannot supply direct information on the orientation of two flexible subunits, but when the conformation is pseudorigid or the linkage of these two six-membered chairlike rings is known, it is still very useful to bridge the relative orientations of two remote bound pairs. Otherwise, order matrix analysis is needed for the total structural information. The combination of RDCs with NOEs and *J* couplings will be an even more powerful approach to solve stereochemical problems.

Conclusion

The collection of C−H RDCs in the direct dimension exploits the inherent high digital resolution of the ^{1}H dimension in HMQC experiments. The effect of the asymmetric line shape in the direct measurement can be minimized by phasing each of the measured satellites independently. It is quick and accurate and can be readily applied to the structural and stereochemical study of small molecules at natural abundance. The multitude of biological or organic liquid crystals, such as 4-cyano-4′-pentyldiphenyl, means that in principle many organic compounds can be aligned and studied using direct measurements.

We have presented a novel method for the determination of the relative stereochemistry of six-membered chairlike ring compounds by investigating the similarity of one-bond C−H/C−X RDCs. It is a simple version of the approaches that have long and successfully been used in the structural determination of macromolecules since data analysis does not rely on mathematical calculation of the molecular order tensor. The similar RDCs of the parallel C−H/C−X vectors, which may not be counted as useful independent constraints for analysis, were used to bridge the relative stereochemistry of protons on the six-membered chairlike ring fragments. While this method is demonstrated on a disaccharide, we propose that the inspection of RDCs allows the relative stereochemistry of any pair of nuclei (H−H, C−H, N−H, C−C, or C−N) in a six-membered chairlike ring to be determined without calculation of the order tensor and more complicated measurements of other types of RDCs. Using RDCs only is a paradigmatic leap for small molecule structure determination and will have major implications in organic chemistry. Instead of multiple connections by NOE and *J* scalar couplings, the measurement of C−H RDCs now allows us to obtain the relative stereochemistry of two remote protons. The advantage of this method is greater if proton linkage between two remote C−H/C−X/X−H bonds is missing.

Experimental Procedure

Materials and NMR Sample Preparation. 4,6-*O*-EGP, F-Glc, and β-lactose (β-D-galactose (1 → 4) β-D-glucose) were available commercially. Pf1 bacteriaphage was prepared and

(46) Duus, J. O.; Gotfredsen, C. H.; Bock, K. Carbohydrate Structural Determination by NMR Spectroscopy: Modern Methods and Limitations. *Chem. Rev. (Washington, D.C.)* **2000**, *100*, 4589−4614.

(47) Jarvis, M. C. Relationship of chemical shift to glycosidic conformation in the solid-state 13C NMR spectra of (1®4)-linked glucose polymers and oligomers: anomeric and related effects. *Carbohydr. Res.* **1994**, *259*, 311−318.

(48) Bradbury, J. H.; Collins, J. G. An approach to the structural analysis of oligosaccharides by NMR spectroscopy. *Carbohydr. Res.* **1979**, *71*, 15−24.

(49) Kreveld, A. V.; Michaels, A. S. Measurement of crystal growth of a-lactose. *J. Dairy Sci.* **1965**, *3*, 259−265.

(50) Engelsen, S.; Rasmussen, K. b-Lactose in the view of a CFF-optimized force field. *J. Carbohydr. Chem.* **1997**, *16*, 773−788.

(51) Oh, J.; Kim, Y.; Won, Y. Conformational analysis and molecular dynamics simulation of lactose. *Bull. Korean Chem. Soc.* **1995**, *16*, 1153−1162.

(52) Ravishankar, R.; Surolia, A.; Vijayan, M.; Lim, S.; Kishi, Y. Preferred Conformation of C-Lactose at the Free and Peanut Lectin Bound States. *J. Am. Chem. Soc.* **1998**, *120*, 11297−11303.

(53) Duda, C. A.; Stevens, E. S. Lactose conformation in aqueous solution from optical rotation. *Carbohydr. Res.* **1990**, *206*, 347−351.

purified as described by Hansen et al.[34] 4,6-*O*-EGP and F-Glc samples were prepared in 1× phosphate-buffered saline (PBS) of 99.9% D_2O (pD 7.30), while β-lactose was dissolved in D_2O (99.9%). Phage pellets was resuspended and pelleted twice into 0.5 mL of PBS buffer or D_2O prior to use. Bicelles containing 1,2-dimyristoyl-*sn*-glycero-3-phosphocholine (DMPC) and 1,2-dihexanoyl-*sn*-glycero-3-phosphocholine (DHPC) (2.8:1 molar ratio) were available commercially.

General NMR Experiments. All NMR experiments were performed on a 600 MHz spectrometer with a 5 mm inverse triple-resonance ($^{15}N/^{13}C/^{1}H$) probe equipped with triple-axis actively shielded gradients. The spectra were processed using Bruker Xwinnmr. As shown in Figure 1, 1D and 2D HMQC[25] spectra were modified slightly to determine the scalar coupling and residual dipolar coupling constants in the ^1H dimension without decoupling in the acquisition period. Splittings were measured as the separation between ^{13}C satellites of a given resonance, and the frequencies of multiples of each satellite were read after the satellite signal was phased independently. One-bond C−H RDC was calculated from the splitting difference between oriented and isotropic signals. DQF-COSY,[54] TOCSY,[55] and NOESY (nuclear Overhauser effect spectroscopy)[56] were all recorded with 1024 × 256 data points to cover a sweep width of 2404 Hz for lactose or 2048 × 256 data points to cover 4808 Hz for 4,6-*O*-EGP. Quadrature indirect detection was achieved through TPPI for these homonuclear correlation experiments. The mixing times for TOCSY and NOESY were 150 ms and 1.2 s, respectively. The recovery delay for all these 2D experiments was 2 s. The 2D homonuclear spectra were processed by applying a cosine squared function to both dimensions prior to zero-filling by a factor of 2 before Fourier transfer.

Residual Dipolar Coupling Measurement of Lactose. An isotropic and two aligned (containing 10 and 14 mg/mL phage, respectively) lactose samples were prepared by diluting or mixing the concentrated lactose solution in D_2O or D_2O-resuspended phage. Deuterium spectra were recorded to check the alignments of the phage samples, and 10.4 and 14.2 Hz splittings were observed, respectively. Experiments for these samples were performed at 298 K. Bicelles were dissolved in 0.5 mL of lactose/D_2O solution and hydrated for overnight at room temperature. Spectra of bicelle samples were recorded at 298 and 319 K for isotropic and oriented measurements, respectively. The concentration of bicelles was about 14% (w/v) and a splitting of 15.6 Hz was obtained in the deuterium spectrum at 319 K. The concentration of lactose in all NMR samples was 300 mM.

The 1D HMQC spectra were acquired with 16K data points over a spectrum width of 2400 Hz for an experimental resolution of 0.29 Hz per point. 2D HMQC spectra were collected with the same parameters as the 1D experiments in the ^1H dimension, while 64 data points were collected for a 3600 Hz spectral width in the ^{13}C dimension. The FID digital resolutions for the ^1H and ^{13}C dimensions are 0.29 and 56.3 Hz per point, resulting in an acquisition time of 160 min. An INEPT delay τ of 3.12 ms corresponding to a J constant of 160 Hz was used. Reduction of the signal-to-noise ratio due to complicated multiplets was observed in the F_2 (^1H) dimension. Since only the one-bond C−H J and D couplings were of interest, an exponential window function with 2 Hz line broadening was applied to the H dimension. A cosine squared function was applied to the ^{13}C dimension prior to zero-filling by a factor of 2 and linear prediction by 50% was applied to the F_1 (^{13}C) dimension before Fourier transformation. 2D CT-HSQC was acquired with 1K × 512 points to cover a spectral window of 2404 Hz × 6037 Hz in F_2 (^1H) and F_1 (^{13}C), resulting in a resolution of 11.8 Hz in F_1. The ^1H and ^{13}C carrier frequencies were centered at HDO and 72 ppm, respectively. A linear prediction by 50% and a zero-filing by a factor of 16 were applied to the ^{13}C dimension before Fourier transformation. From 1D and 2D HMQC experiments, frequencies of multiplets of each ^{13}C satellite of a given resonance were measured after the satellite signal was phased independently. The signal frequencies on the CT-HSQC were determined by automatic peak-picking.

Residual Dipolar Coupling Measurement of 4,6-*O*-EGP. The aligned 4,6-*O*-EGP sample was prepared by mixing the 358 mM 4,6-*O*-EGP PBS solution in resuspended phage. The final concentration of 4,6-*O*-EGP was 10 mM, and a 13.5 Hz splitting was observed in the deuterium spectrum. An identical isotropic sample was also made to measure the isotropic J couplings. 2D HMQC spectra for dipolar measurement were collected with 32k × 64 points to cover a spectral window of 4808 Hz × 3320 Hz in F_2 (^1H) and F_1 (^{13}C), resulting in the FID resolutions of 0.15 and 51.9 Hz in F_2 and F_1, respectively. An INEPT delay τ of 3.12 ms corresponding to a J constant of 160 Hz was used. An exponential window function with 2 Hz line broadening was applied to the F_2 (^1H) dimension to decrease the loss of signal-to-noise ratio caused by complicated multiple splitting from long-range H−H interaction. A zero-filling by a factor of 2 before Fourier transformation was also used in this dimension. A linear prediction by 50% and a zero-filing by a factor of 4 were applied to the F_1 (^{13}C) dimension.

Residual Dipolar Coupling Measurement of F-Glc. Isotropic and phage-aligned F-Glc samples were made in the same way described above; the F-Glc concentration was 20 mM, and a 16 Hz HOD splitting was measured with the aligned F-Glc sample. C−H RDCs were measured by 2D HMQC spectra collected with 12k × 32 points to cover a spectral window of 2000 Hz × 1500 Hz in F_2 (^1H) and F_1 (^{13}C), resulting in FID resolutions of 0.15 and 47.2 Hz in F_2 and F_1, respectively. An INEPT delay τ of 3.12 ms corresponding to a J constant of 160 Hz was used. Before Fourier transformation an exponential window function with 2 Hz line broadening and a zero-filling by a factor of 2 were applied to the F_2 (^1H) dimension and a linear prediction by 50% and a zero-filing by a factor of 4 to the F_1 (^{13}C) dimension. C−F RDCs were measured by 1D NOE-enhanced ^{13}C experiments. A spectral width of 22900 Hz was covered by 80K points, resulting in a 0.28 Hz FID resolution. An exponential window function with 1 Hz line broadening and a zero-filling by a factor of 2 were applied before Fourier transformation.

JO020670I

(54) Derome, A.; Williamson, M. *J. Magn. Reson.* **1990**, *88*, 177−185.
(55) Shaka, A. J.; Lee, C. J.; Pines, A. *J. Magn. Reson.* **1988**, *77*, 274.
(56) Jeener, J.; Meier, B. H.; Bachmann, P.; Ernst, R. R. Investigation of exchange processes by two-dimensional NMR spectroscopy. *J. Chem. Phys.* **1979**, *71*, 4546−4553.